Crystal structure of haloalkane dehalogenase

Franken, Sybille M.; Rozeboom, Henriette; Kalk, Kor H.; Dijkstra, Bauke W.

Published in:
Default journal

Publication date:
1991

The EMBO Journal vol.10 no.6 pp.1297-1302, 1991

Crystal structure of haloalkane dehalogenase: an enzyme to detoxify halogenated alkanes

Sybille M.Franken[1], Henriette J.Rozeboom, Kor H.Kalk and Bauke W.Dijkstra

Laboratory of Chemical Physics, Department of Chemistry, Nijenborgh 16, 9747 AG Groningen, The Netherlands

[1]Present address: Max-Planck Institut für medizinische Forschung, Abt. Biophysik, Jahnstr. 29, D-6900 Heidelberg, FRG

Communicated by W.G.J.Hol

Haloalkane dehalogenase from *Xanthobacter autotrophicus* GJ10 converts 1-haloalkanes to the corresponding alcohols and halide ions with water as the sole cosubstrate and without any need for oxygen or cofactors. The three-dimensional structure has been determined by multiple isomorphous replacement techniques using three heavy atom derivatives. The structure has been refined at 2.4 Å resolution to an *R*-factor of 17.9%. The monomeric enzyme is a spherical molecule and is composed to two domains: domain I has an α/β type structure with a central eight-stranded mainly parallel β-sheet. Domain II lies like a cap on top of domain I and consists of α-helices connected by loops. Except for the cap domain the structure resembles that of the dienelactone hydrolase in spite of any significant sequence homology. The putative active site is completely buried in an internal hydrophobic cavity which is located between the two domains. From the analysis of the structure it is suggested that Asp124 is the nucleophilic residue essential for the catalysis. It interacts with His289 which is hydrogen-bonded to Asp260.

Key words: haloalkane dehalogenase/1-haloalkanes/nucleophilic substitution/X-ray protein structure

Introduction

Haloalkane dehalogenase is an enzyme isolated from the nitrogen-fixing bacterium *Xanthobacter autotrophicus* GJ10 (Janssen *et al.*, 1985). This organism is able to grow on 1,2-dichloroethane as a sole carbon and energy source. The first step in the organism's degradation of 1,2-dichloroethane is a hydrolytic dehalogenation which is catalysed by haloalkane dehalogenase. A chloride ion and the corresponding alcohol are released.

$$Cl\text{-}CH_2\text{-}CH_2\text{-}Cl + H_2O \rightarrow Cl\text{-}CH_2\text{-}CH_2\text{-}OH + H^+ + Cl^-$$

The enzyme has a molecular weight of 35 kd and consists of 310 amino acid residues. The nucleotide sequence is known (Janssen *et al.*, 1989). Because neither oxygen nor cofactors are needed for the reaction catalysed by haloalkane dehalogenase a nucleophilic substitution with water has been suggested as the reaction mechanism (Janssen *et al.*, 1988). The enzyme's activity is strongly inhibited by thiol reagents such as $HgCl_2$, iodoacetamide and *p*-chloromercuribenzoate (Keuning *et al.*, 1985). Four cysteine residues have been found in the amino acid sequence and it has been hypothesized that one of these cysteines takes part in the reaction mechanism (Keuning *et al.*, 1985), possibly following a reaction mechanism involving a thioether as proposed by Goldman (1965).

Substrates for the enzyme are terminally halogenated alkanes with chain lengths of up to four carbon atoms for 1-chlorinated alkanes and up to at least 10 carbon atoms for 1-brominated alkanes (Janssen *et al.*, 1989). A number of these halogenated aliphatic compounds are industrially produced in large amounts for use as solvents, cleaning agents, pesticides and as intermediates for chemical syntheses. They are also a major class of environmental pollutants. Enzymes like haloalkane dehalogenase offer a very elegant way to detoxify media biologically, which are contaminated with these xenobiotics. However, the affinity of the enzyme towards its substrates is not very high (K_m = 1.1 mM), the turnover number is low (k_{cat} = 6 s^{-1}) and the substrate range is limited (Keuning *et al.*, 1985). Thus haloalkane dehalogenase is a challenging target for protein engineering towards a practical 'antipollutant' with improved activity and broadened or altered substrate specificity. The three-dimensional structure of the enzyme, which is presented here, may serve as a basis for site-directed mutagenesis experiments and could in addition help in the understanding of the enzyme's intriguing reaction mechanism.

Results

Crystallography

The molecular model of haloalkane dehalogenase presented here consists of the amino acids 3-307 and includes 110 water molecules. No electron density is visible for the first two N-terminal and the three C-terminal residues 308-310. The rest of the main chain allowed an unambiguous tracing. The present crystallographic *R*-factor for all observed 11 272 reflections between 2.4 and 7 Å is 17.9% ($R = \Sigma||F_o|-|F_c||/\Sigma|F_o|$). The r.m.s. deviations from ideal geometry are 0.007 Å for bond lengths and 2.9° for bond angles. The estimated coordinate error from a σ_A plot is 0.18 Å (Read, 1986).

Overall structure

Haloalkane dehalogenase has a globular shape with overall dimensions of about 49 × 52 × 43 $Å^3$. The molecule is composed of two domains (as shown in Figure 1). Domain I comprises the residues 1-155 and 230-310 and shows the typical features of an α/β type protein. It consists of a central eight-stranded β-pleated sheet with seven parallel strands. This sheet is flanked on both sides by α-helices, two are on one side and four are on the other side of the sheet. As can be seen in Figure 1b, the typical $\beta-\alpha-\beta$ connectivity (Sternberg and Thornton, 1977) is followed in

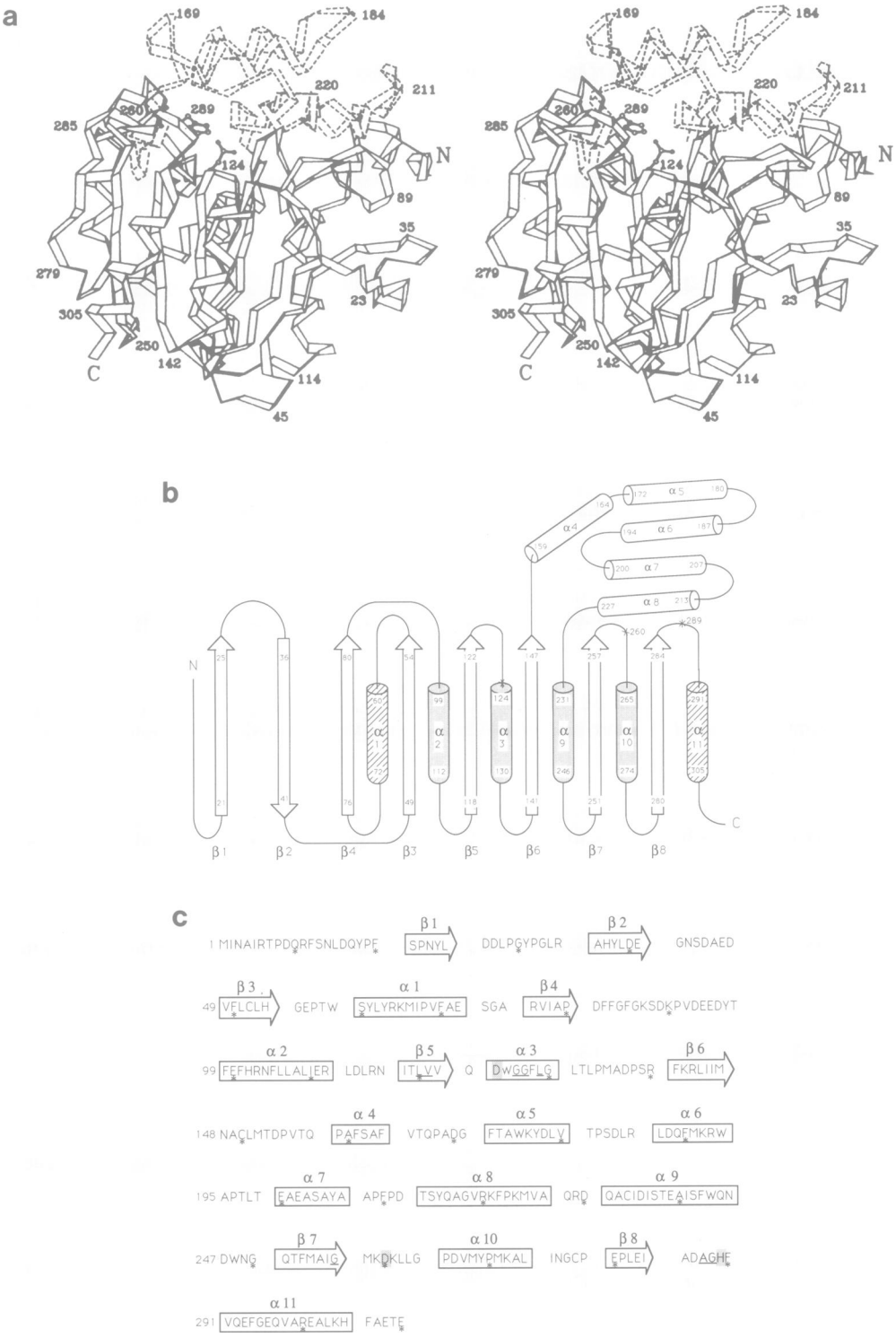

Fig. 1. (**a**) Stereoview of the α-carbon chain. Domain I is drawn with solid lines and domain II with dashed lines. The putative active site residues are indicated. Selected residues are labelled. (**b**) Topology of the secondary structure elements [as determined by the program DSSP (Kabsch and Sander, 1983)]. α-helices are represented as cylinders and β-strands as arrows. Helices on the one side of the β-sheet are dashed, the ones on the other side are shaded and the ones of domain II are unfilled. The numbers of the first and last residues of each secondary structural element are included and the position of the three putative active site residues are marked with an asterisk (*). (**c**) Single letter coded amino acid sequence (Janssen *et al.*, 1989), showing the positions of the α-helices (rectangles) and β-strands (arrows). Every 10th residue is marked with an asterisk and the putative active site residues (Asp124, Asp260, His289) are shaded. The residues which are identical to the ones in dienelactone hydrolase (DLH, Pathak *et al.*, 1988) are underlined.

strands 3−8 with all crossover connections being right-handed (Richardson, 1976). There are, however, deviations from the β−α−β connectivity at strands 1, 2 and 3: strand 1 is connected to the single antiparallel strand 2 through a tight turn and strand 2 leads via a loop directly into strand 3. Domain II (residues 156−229) lies like a cap on top of domain I and consists of five α-helices which are connected by loops. This domain forms an extraordinarily long connection between strands 6 and 7 of domain I. The strand order of the α/β unit formed by the strands 3−8 is 213456.

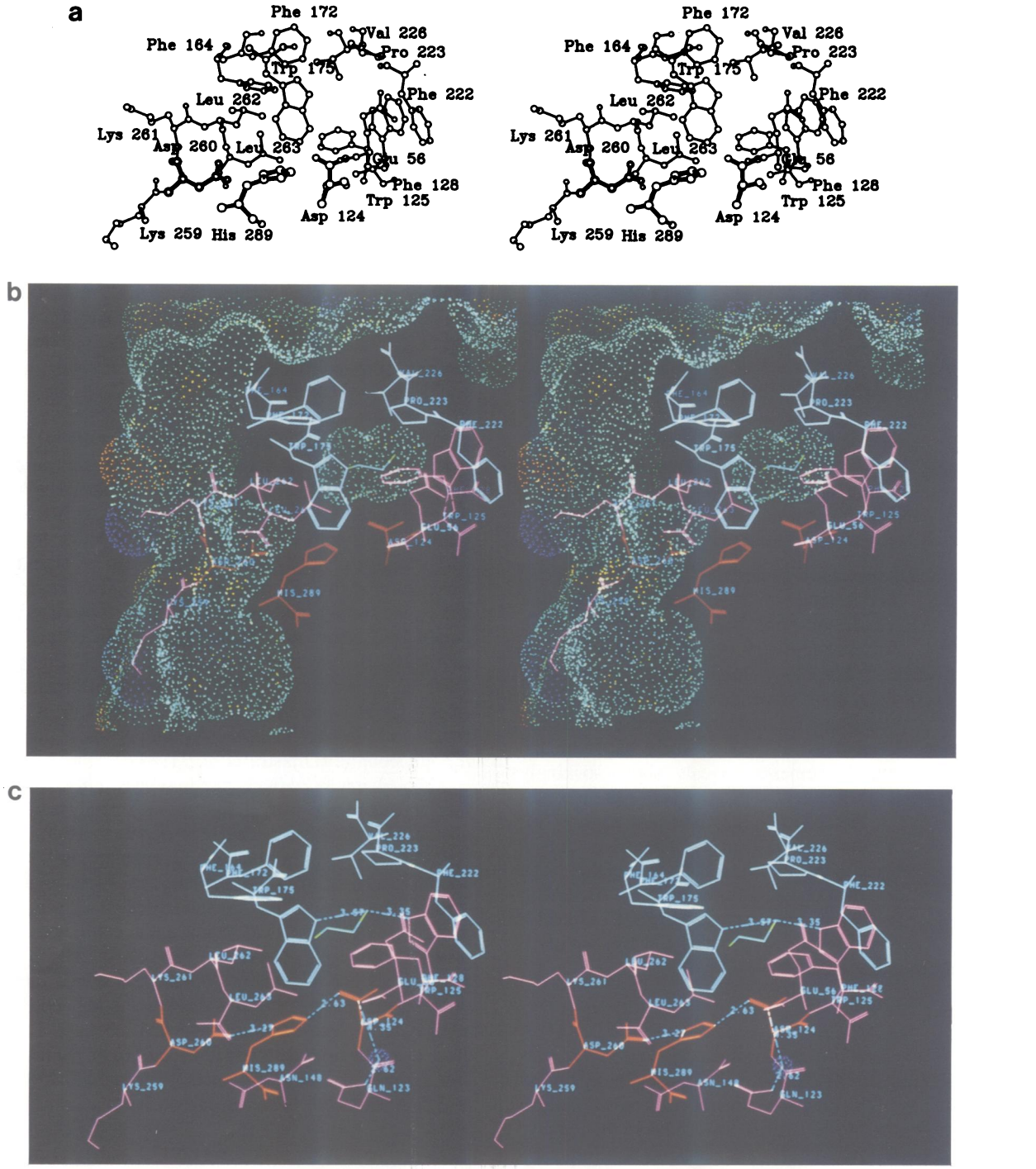

Fig. 2. Active site of dehalogenase. (**a**) Stereo picture of the residues which make up the internal cavity. The three residues which are probably involved in the reaction are emphasized using heavier lines. (**b**) As (a) with a calculated molecular surface (dotted and coloured according to charge: blue = positively charged, green = neutral and red = negatively charged). This protein surface can be seen facing towards the left and upper edges of this view, with the tunnel extending towards the centre from the lower left. The cavity near the centre is almost connected to the tunnel. The tunnel entrance is flanked by two lysine residues (Lys259 and Lys261). Residues from domain I are shown in pink and from domain II in light blue, the residues involved in activity in red. 1,2-dibromoethane (blue-green) as a substrate is docked in the cavity. (**c**) As (b) and including residues Glu123, Asn148 and the water molecule close to Glu123 (blue dotted surface). The colour coding is the same as in (b). Distances between selected residues are indicated in Å.

The active site

Assuming that a cysteine residue could be involved in the reaction mechanism (Keuning *et al.*, 1985), the environment of the four cysteines was carefully examined to find the active site. However, we could not find any obvious depressions or crevices near the cysteines or elsewhere on the surface of the protein, which could take up a substrate molecule. Instead, an internal cavity of ~40 Å^3 size was found (see Figure 2). It is positioned between the two domains: domain I contributes side chains of residues from the carboxy termini of strands 3, 7 and 8 and from helix 3 to the lining of the cavity. These residues are Glu56, Leu262, Leu263, His289, Asp124, Trp125 and Phe128. The cavity is further covered by helices 4, 5 and 8 of domain II (residues Phe164, Phe172,

Trp175, Phe222, Pro223 and Val226). A tunnel extends towards the cavity from the solvent region (see Figure 2b). This tunnel appears to be blocked from reaching the cavity by leucine 262. However, even in the crystalline state this leucine must be flexible, because it was found that the gold cyanide molecule (soaked into the crystal as a heavy atom derivative) was bound in this internal cavity. In the native structure two water molecules are bound in the cavity.

As depicted in Figure 2 the residues composing this cavity are mainly hydrophobic. Asp124 is the only charged residue which points into the cavity. Oδ2 of Asp124 is hydrogen bonded to two main chain nitrogen atoms (124Oδ2...N56 3.0 Å, 124Oδ2..N125 2.6 Å). Oδ1 of Asp124 is 2.6 Å away from Nε2 of His289. The Nδ1 of His289 can interact with Oδ1 of Asp260 (289Nδ1...260Oδ1 3.3 Å) (see also Figure 2c). This aspartate 260 points into the interior of the protein in spite of its polar character. Its side chain makes further hydrogen bonds with the side chain of Asn148 (260Oδ1...148Nδ1 2.8 Å) and with the main chain nitrogen atoms of residues Leu262 and Leu263 (260Oδ2...N262 3.1 Å, 260Oδ1...N263 2.9 Å). His289 and Asp260 line the tunnel which leads towards the cavity.

Similarity to dienelactone hydrolase

Surprisingly, the folding of haloalkane dehalogenase resembles that of dienelactone hydrolase (DLH, Pathak *et al.*, 1988; Pathak and Ollis, 1990) in spite of any significant sequence homology (Janssen *et al.*, 1989). The arrangement of the β-sheet is identical in both enzymes, but DLH is missing the entire cap domain and has instead only a short loop. A sequence alignment solely based on the secondary structural elements reveals short strikingly homologous stretches around the putative active site residues of DLH (Asp171, His202, Cys123) (see also Figure 1c). Residues Asp260 and His289 of dehalogenase are at equivalent positions to Asp171 and His202 of DLH. The active site cysteine 123 of DLH is replaced by Asp124 in dehalogenase. The two residues preceding His289 (Ala287, Gly288) are identical in the two proteins and five out of 10 residues surrounding Asp124.

Discussion

The two-domain structure of haloalkane dehalogenase reveals an internal hydrophobic cavity which is completely buried between the two domains. For several reasons we believe that the active site of the enzyme is located in this cavity.

The cavity has a perfect size and shape to accommodate molecules like the main substrates 1,2-dichloroethane and 1,2-dibromoethane (Keuning *et al.*, 1985) as could be shown in docking experiments (see also Figure 2b).

Gold cyanide can be bound in the cavity. It has been shown that large complex anions like $[Au(CN)_2]^-$ act as competitors towards halogen ions for the high affinity anion binding sites of proteins (Norne *et al.*, 1975). In fact during the reaction of dehalogenase a halide ion is produced which has to be stabilized in order to facilitate the reaction. In addition, $[Au(CN)_2]^-$ readily inhibits the enzyme in solution (D.B.Janssen, personal communication).

The position of the cavity agrees with the observation of Brändén (1980) that substrate binding crevices often occur at strand order switch points. In dehalogenase such a strand order switch point is at the carboxyl ends of strands 3 and 5. This position resembles closely the position of the substrate binding cleft in dienelactone hydrolase (Pathak *et al.*, 1985). In DLH however, the cleft is at the surface of the molecule and partly exposed to the solvent. A flap-like domain forms one of the walls of the active site cleft. In dehalogenase the cap domain shields the cleft entirely from the solvent region and provides a hydrophobic cavity. This arrangement is comparable with that in lipase, where the active site is buried under a long loop (Brady *et al.*, 1990; Winkler *et al.*, 1990). Whereas in the lipases substantial conformational changes have to take place before the bulky substrate can bind in the active site (Winkler *et al.*, 1990), in dehalogenase probably only minor rearrangements at the tunnel entrance are necessary in order to make the active site accessible for the much less bulky 1-haloalkanes. These rearrangements are even possible in the crystalline state where $[Au(CN)_2]^-$ could be soaked into the cavity yielding an excellent isomorphous derivative (Table II).

As was pointed out above, the internal cavity is lined with hydrophobic residues and a substrate molecule could nicely be fitted in it by docking experiments. Asp124 is the only charged residue which is close to the cavity. It is at a similar position to the active site cysteine in dienelactone hydrolase. The negative charge of the aspartate can be stabilized by its position at the N-terminus of a helix (Hol *et al.*, 1978) and by interactions with His289 which itself can interact with Asp260 (see above and Figure 2c). Asp/His couples similar to Asp260/His289 have been found in lipases (Brady *et al.*, 1990; Winkler *et al.*, 1990) and serine proteases (Blow *et al.*, 1969), where the attacking nucleophile is a serine residue and in phospholipase A_2 with a water molecule as the nucleophile (Dijkstra *et al.*, 1981).

Although it may be premature to suggest a detailed reaction mechanism of the hydrolytic cleavage catalysed by haloalkane dehalogenase, it seems reasonable to assume that the reaction occurs via a nucleophilic substitution with either an amino acid side chain of the enzyme or with an activated water molecule acting as the nucleophile (see e.g. Janssen *et al.*, 1988). Amino acid residues that could activate such a water molecule could be Asp124 or His289. Both possibilities seem unlikely because the above mentioned docking experiments indicate that there is not enough room for a water molecule near the modelled substrate. Therefore, from our structural data Asp124 seems to be the most likely candidate as the attacking nucleophile, as its Oδ1 atom is ~3.5 Å from the attacked carbon atom of the modelled substrate.

Two tryptophane residues (Trp125 and 175) point with their ring nitrogen atoms towards the cavity in such a way that they could stabilize the resulting halide ion as well as a negatively charged five-coordinated carbon in the transition state (as occurring in a bimolecular nucleophilic substitution). The assumed covalent intermediate would be an ester which must subsequently be cleaved by a water molecule, releasing the alcohol. At the current resolution one water molecule can be localized at a distance of 4.5 Å from the Cγ of Asp124 and bound to Oε1 of Glu123 which points into the direction of Asp124 (Figure 2c). Studies at higher resolution might reveal the positions of water molecules in more detail.

Other mechanisms such as e.g. a β-anti-elimination or an electrophilic substitution with a metal ion in the active site have been proposed (see e.g. Janssen *et al.*, 1988) but most of these are incompatible with either the properties of haloalkane dehalogenase or the architecture of its active site.

Table I. Data collection and processing

Data set	native	$K_2[PtCl_4]$	$UO_2(NO_3)_2$	$Na[Au(CN)_2]$
No. of crystals	2	1	1	1
No. of measurements	52 590	21 645	26 231	34 819
No. of unique reflections	11 506	7060	7646	9467
Max. resolution (Å)	2.30	2.44	2.45	2.48
R_{merge}[a]	8.04 (on I)	7.4 (on F)	4.83 (on F)	5.57 (on F)
R_{PH}[b] (%)	–	17.1	14.0	17.0
Completeness to 2.7 Å (%)	97	76	82	93

[a] $R_{merge} = \Sigma|I_i^h + <I^h>|/\Sigma<I^h>$
[b] $R_{PH} = \Sigma|F_{PH} - F_P|/\Sigma_{FP}$

Table II. Multiple isomorphous refinement statistics

Resolution (Å)	11.11	7.69	5.88	4.76	4.00	3.44	3.03	2.70	total
No. of reflections	104	251	457	696	1000	1347	1756	2092	7703
Figure of merit	0.74	0.80	0.81	0.79	0.73	0.71	0.67	0.58	0.69
$K_2[PtCl_4]$									
No. of reflections	85	192	393	601	808	1113	400	–	3592
Rc (%)[a]	50.52	62.47	77.24	82.76	82.86	79.47	81.99	–	73.23
Phasing power[b]	1.34	1.97	1.94	1.60	1.20	1.08	1.00	–	1.37
$UO_2(NO_2)_2$									
No. of reflections	–	38	391	606	863	1204	1227	–	4337
Rc (%)[a]	–	76.17	87.94	75.65	79.29	77.94	82.62	–	80.43
Phasing power[b]	–	1.11	1.17	1.31	1.01	1.13	1.06	–	1.11
$Na[Au(CN)_2]$									
No. of reflections	77	238	429	655	940	1296	1726	2092	7453
Rc (%)[a]	28.33	35.61	34.99	50.20	58.07	54.13	54.11	52.89	49.44
Phasing power[b]	3.78	3.10	3.70	2.96	2.59	2.44	2.55	2.45	2.64

[a] $Rc = \Sigma||F_{PH}| - |F_P + F_H||/\Sigma||F_{PH}| - |F_{PH}||$ for centric reflections
[b] Phasing power is the ratio of the r.m.s. heavy atom scattering factor amplitude to the r.m.s. lack of closure error

The structural information also seems to rule out that a cysteine is involved in the reaction mechanism, since the closest cysteine (Cys150) is 8.5 Å away from the cavity and it is shielded by Phe 128. The inhibition of the enzyme by thiol reagents might be due to conformational changes which could disturb or even destroy the perfectly fitting hydrophobic cavity or the arrangement of catalytic residues. Crystals which were soaked in mercury-containing solutions cracked or did not diffract any more, suggesting that conformational changes occurred.

It is clear that more research is needed to validate our proposed reaction mechanism. First attempts to bind substrate analogues in the crystals have been unsuccessful. Also site-directed mutagenesis will be used to determine whether the proposed active site residues are indeed essential for activity. In addition it will be most exciting to see how the substrate specificity can be altered by protein engineering techniques.

Materials and methods

Crystal structure determination

Purified haloalkane dehalogenase has been crystallized in hanging drops from a bis-Tris–H_2SO_4 buffer solution [bis(2-hydroxyethyl)-imino-tris(hydroxymethyl)methane] of pH 5.8–6.4 using ammonium sulphate as a precipitant (Rozeboom *et al.*, 1988). The best crystals were obtained from a 64% saturated $(NH_4)_2SO_4$ solution at pH 6.2. These crystals are of space group $P2_12_12$ with unit cell dimensions of a = 94.8 Å, b = 72.8 Å and c = 41.4 Å. The asymmetric unit contains one monomeric molecule with a molecular weight of 35 kd. The estimated solvent content is 39%.

Heavy atom derivatives were prepared by soaking native crystals in the corresponding heavy atom solution. Considering the existence of four cysteine residues in the amino acid sequence (Janssen *et al.*, 1989), ~10 different mercury compounds were tried in various concentrations. None of these trials, however, yielded a useful derivative, but instead the crystals either cracked or did not diffract any more. Three other derivatives were found to be useful: 1 mM $K_2[PtCl_4]$, 3 mM $UO_2(NO_3)_2$ and 3 mM $Na[Au(CN)_2]$, all soaked for 1 day.

X-ray diffraction data for the native enzyme and the heavy atom derivatives were collected at room temperature on a FAST area detector (Enraf Nonius, Delft, The Netherlands) using Cu-K_α radiation. The X-ray source was an Elliot GX21 rotating anode X-ray generator with a Huber graphite monochromator. The intensities were collected in frames of 0.1°–0.15° using two different crystal settings for each crystal.

Data were processed on-line using the MADNES system (Messerschmidt and Pflugrath, 1987) and for some data sets applying the Kabsch profile fitting procedure (Kabsch, 1988). Subsequently the data were processed using a standard program set of the Groningen BIOMOL crystallographic software package.

Both three-dimensional difference Patterson maps (3–15 Å resolution) of the Au and Pt derivatives were readily interpretable in terms of one major site per derivative. A uranyl site as well as a second platinum site could be localized in cross difference Fourier maps. The heavy atom parameters

were refined using the program PHARE (Bricogne, 1976), including the anomalous contributions of all three derivatives and yielding an overall figure of merit of 0.69.

With these 'best phases' a 2.7 Å Fourier map was calculated. The molecular boundaries of four molecules in the unit cell could clearly be recognized. A molecular envelope was calculated (Leslie, 1987), applying an integration radius of 7 Å and a value of the solvent content of 32%, which is slightly smaller than the calculated value (39%). This envelope was checked to avoid cutting off part of the protein molecule and it was not updated during the solvent flattening procedure (Wang, 1985). The resulting phases of each cycle were combined with the ones from the previous cycle. After 14 cycles the final figure of merit was 0.82 and the overall phase shift was 28.1° for 8288 reflections [including observed reflections which did not have an original phase from multiple isomorphous replacement (MIR)].

The electron density map calculated with these modified phases was stacked on plexiglass sheets and a part of the polypeptide backbone was traced. C_α coordinates were measured and transferred to the program WHATIF (Vriend, 1990), which converted the C_α coordinates into a poly-alanine chain. This chain was fitted into the electron density using the graphics program FRODO (Jones, 1978) on an Evans & Sutherland PS390 computer graphics system. Side chains could be recognized by their shape and could be correlated to the amino acid sequence (Janssen *et al.*, 1989). Residues 35–307 could be traced unambiguously, but the stretch 1–34 remained unclear. To solve this problem phases from the 90% complete model were calculated and they were combined with the original MIR phases, using the weighting scheme of the program SIGMAA (Read, 1986). The new electron density calculated with these combined phases was much clearer and the amino acids 3–34 could easily be traced.

The refinement of the model was carried out on a VAX3200 using the program TNT (Tronrud *et al.*, 1987). Isotropic temperature factors were initially set to 15 $Å^2$ and they were only refined in the later stages of the refinement. Occupancies were set to unity and were not refined. At intervals the model was inspected and rebuilt where necessary. Electron density maps were calculated with coefficients $(2mF_0-DF_c(\exp(i\alpha_c)$ to minimize model bias (Read, 1986). Solvent molecules were placed by searching σ_A-weighted (F_0-F_c) maps for peaks (Read, 1986). Peaks too close to the protein or further than 3.5 Å from the protein or other solvent molecules were rejected. The starting *R*-factor was 40.8% in a resolution range of 3–7 Å. The resolution was gradually extended to 2.4 Å and the *R*-factor improved with progressing refinement to 17.9%.

Coordinates of the refined structure have been deposited with the Protein Data Bank (Bernstein *et al.*, 1977).

Acknowledgements

We thank Dr D.B.Janssen and coworkers for their ample supply of protein material and many stimulating discussions. Help and advice from, and numerous discussions with, many members of the Groningen Protein Crystallography Group are gratefully acknowledged, in particular the docking experiments by Dr C.Verlinde. Computational and computer graphics facilities were provided by the BIOSON Research Institute. Supported by the Programma Commissie voor Biotechnologie (PCB) of the Ministry of Economic Affairs.

References

Bernstein,F.C., Koetzle,T.F., Williams,G.J.B., Meyer Jr.,E.F., Brice,M.D., Rodgers,J.R., Kennard,O., Shimanouchi,T. and Tasumi,M. (1977) *J. Mol. Biol.*, **112**, 535–542.

Blow,D.M., Birktoft,J.J. and Hartley,B.S. (1969) *Nature*, **221**, 337–340.

Brady,L., Brzowski,A.M., Derewenda,Z.S., Dodson,E., Dodson,G., Tolley,S., Turkenburg,J.P., Christiansen,L., Huge-Jensen,B., Norskov,L., Thim,L. and Menge,U. (1990) *Nature*, **343**, 767–770.

Brändén,C.I. (1980) *Quart. Rev. Biophys.*, **13**, 317–338.

Bricogne,G. (1976) *Acta Crystallog. A*, **32**, 832–847.

Dijkstra,B.W., Drenth,J. and Kalk,K.H. (1981) *Nature*, **289**, 604–606.

Goldman,P. (1965) *J. Biol. Chem.*, **240**, 3434–3438.

Hol,W.G.J., van Duijnen,P.T. and Berendsen,H.J.C. (1978) *Nature*, **273**, 443–446.

Janssen,D.B., Scheper,A., Dijkhuizen,L. and Witholt,B. (1985) *Appl. Environ. Microbiol.*, **49**, 673–677.

Janssen,D.B., Gerritse,J., Brackman,J., Kalk,C., Jager,D. and Witholt,B. (1988) *Eur. J. Biochem.*, **171**, 67–72.

Janssen,D.B., Pries,F., van der Ploeg,J., Kazemier,B., Terpstra,P. and Witholt,B. (1989) *J. Bacteriol.*, **171**, 6791–6799.

Jones,T.A. (1978) *J. Appl. Crystallogr.*, **11**, 268–272.

Kabsch,W. (1988) *J. Appl. Crystallogr.*, **21**, 916–924.

Kabsch,W. and Sander,C. (1983) *Biopolymers*, **22**, 2577–2657.

Keuning,S., Janssen,D.B. and Witholt,B. (1985) *J. Bacteriol.*, **163**, 635–639.

Leslie,A.G.W. (1987) *Acta Crystallogr. A*, **43**, 134–136.

Messerschmidt,A. and Pflugrath,J.W. (1987) *J. Appl. Crystallogr.*, **20**, 306–315.

Norne,J.-E., Lilja,H., Lindman,B., Einarsson,R. and Zeppezauer,M. (1975) *Eur. J. Biochem.*, **59**, 463–473.

Pathak,D. and Ollis,D. (1990) *J. Mol. Biol.*, **214**, 497–525.

Pathak,D., Ngai,K.L. and Ollis,D. (1988) *J. Mol. Biol.*, **204**, 435–445.

Read,R.J. (1986) *Acta Crystallogr. A*, **42**, 140–149.

Richardson,J. (1976) *Proc. Natl. Acad. Sci. USA*, **73**, 2619–2623.

Rozeboom,H.J., Kingma,J., Janssen,D.B. and Dijkstra,B.W. (1988) *J. Mol. Biol.*, **200**, 611–612.

Sternberg,M.J.E. and Thornton,J.M. (1977) *J. Mol. Biol.*, **110**, 269–283.

Tronrud,D.E., ten Eyck,L. and Matthews,B.W. (1987) *Acta Crystallogr. A*, **43**, 489–501.

Vriend,G. (1990) *J. Mol Graphics*, **8**, 52–56.

Wang,B.C. (1985) *Methods Enzymol.*, **115**, 90–112.

Winkler,F.K., D'Arcy,A. and Hunziker,W. (1990) *Nature*, **343**, 771–774.

Received on January 14, 1991; revised on March 4, 1991